



HAL
open science

Passive larval transport explains recent gene flow in a Mediterranean gorgonian

Mariana Padrón, Federica Costantini, Sandra Baksay, Lorenzo Bramanti,
Katell Guizien

► **To cite this version:**

Mariana Padrón, Federica Costantini, Sandra Baksay, Lorenzo Bramanti, Katell Guizien. Passive larval transport explains recent gene flow in a Mediterranean gorgonian. *Coral Reefs*, 2018, 37 (2), pp.495-506. 10.1007/s00338-018-1674-1 . hal-02379119

HAL Id: hal-02379119

<https://hal.science/hal-02379119v1>

Submitted on 2 Dec 2022

HAL is a multi-disciplinary open access archive for the deposit and dissemination of scientific research documents, whether they are published or not. The documents may come from teaching and research institutions in France or abroad, or from public or private research centers.

L'archive ouverte pluridisciplinaire **HAL**, est destinée au dépôt et à la diffusion de documents scientifiques de niveau recherche, publiés ou non, émanant des établissements d'enseignement et de recherche français ou étrangers, des laboratoires publics ou privés.

1 **Larval transport explains contemporary gene flow in a Mediterranean gorgonian**

2

3 Mariana Padrón¹, Federica Costantini², Sandra Baksay³, Lorenzo Bramanti¹, Katell Guizien^{1*}

4 ¹ Sorbonne Universités, UPMC Univ Paris 06, CNRS, Laboratoire d'Ecogéochimie des
5 Environnements Benthiques (LECOB), Observatoire Océanologique, 66650, Banyuls sur Mer,
6 France.

7 ² Dipartimento di Scienze Biologiche, Geologiche ed Ambientali (BiGeA) & Centro
8 Interdipartimentale di Ricerca per le Scienze Ambientali (CIRSA), Università di Bologna, ULR
9 CoNISMa, Via S. Alberto 163, I-48123 Ravenna, Italy.

10 ³ Laboratoire Evolution et Diversité Biologique EDB, CNRS, Université Toulouse III Paul
11 Sabatier, F-31062 Toulouse, France.

12

13 *Corresponding author: tel: +33 468887319; e-mail: guizien@obs-banyuls.fr;

14 ORCID: 0000-0001-9884-7506

15

16

17 **Keywords: marine connectivity, Pelagic Larval Duration, genetic structure, Marine**
18 **Protected Areas, hydrodynamic model, Gulf of Lion.**

19

20

21

22

23

24

25

26

27 **Abstract**

28 Understanding the patterns of connectivity is required by the Strategic Plan for Biodiversity
29 2011-2020 and will be used to guide the extension of marine protection measures. Despite the
30 increasing accuracy of ocean circulation modeling, the capacity to forecast the population
31 connectivity of sessile benthic species with dispersal larval stages can be limited due to the
32 potential effect of demographic filters acting before or after dispersal, which modulate offspring
33 release or settlement, respectively. We applied an interdisciplinary approach that combined
34 demographic surveys, genetic methods (assignment tests and coalescent-based analyses) and
35 larval transport simulations to test the relative importance of demographics and ocean currents in
36 shaping the contemporary patterns of gene flow among populations of a Mediterranean gorgonian
37 (*Eunicella singularis*) in a fragmented rocky habitat (Gulf of Lion, NW Mediterranean Sea). We
38 show that larval transport is a dominant driver of gene flow among the populations, and
39 significant correlations were found between the contemporary gene flow and recent larval
40 transport when the pelagic larval durations (PLDs) ranged from 7 to 14 days. Our results suggest
41 that PLDs that efficiently connect populations distributed over a fragmented habitat are filtered
42 by the habitat layout within the species competency period. Moreover, a PLD ranging from 7 to
43 14 days is sufficient to connect the fragmented rocky substrate of the Gulf of Lion. The rocky
44 areas located in the center of the Gulf of Lion, which are currently not protected, were identified
45 as essential hubs for the distribution of migrants in the region. We encourage the use of a range of
46 PLDs instead of a single value when estimating larval transport with biophysical models to
47 identify potential connectivity patterns among a network of marine protected areas or even solely
48 a seascape.

49

50 **Introduction**

51 The Strategic Plan for Biodiversity 2011-2020 aims to conserve 10% of the ocean
52 through well-connected systems of marine protected areas (MPAs) by 2020 (Aichi Target 11,

53 <https://www.cbd.int/sp/targets/rationale/target-11/>). Hence, understanding the degree and patterns
54 of connectivity among existing MPAs and areas where protection could be extended becomes
55 urgent. Connectivity is also known as the mechanism through which populations of sessile marine
56 species, and particularly coral species, can recover after local and global disturbances (Roberts
57 1997; Hanski 1998; Cowen et al. 2000). In the context of global change, relating contemporary
58 connectivity to the seascape processes that shape the spatial distribution of marine species is
59 essential for the design of effective biodiversity conservation strategies.

60 Seascape processes that drive population connectivity of sessile species with a larval
61 dispersal stage, such as corals or gorgonians, should include both seabed geomorphology and
62 dynamic hydrography (Manderson 2016). Correlations at the local scale between demographic
63 population descriptors and the environment may, indeed, not be sufficient, and the successful
64 exchange of individuals between distant locations (i.e., connectivity) should be included. Recent
65 studies on seascape connectivity have focused on evaluating how larval transport drives genetic
66 patterns across the seascape using a combination of biophysical and genetic approaches (see
67 Liggins et al. 2013 for a review). Nonetheless, Selkoe et al. (2016) reported that only 31% of the
68 analyzed studies found ocean currents to be a good predictor of gene flow patterns and ascribed
69 this poor predictability to inappropriate scales in genetic sampling. These findings suggest that
70 demographic and genetic connectivity of benthic sessile species, for which connectivity among
71 populations only occurs during the larval dispersive stage, are affected by several processes
72 acting as successive biological filters at different temporal and spatial scales along their life
73 cycles from spawning to reproduction by the settled individuals (Pineda 2007).

74 Prior to dispersal, population size and fecundity are among the key factors that determine
75 the number of emigrant offspring and have been shown to influence connectivity patterns in
76 marine species (Treml et al. 2012; Dawson et al. 2014). After dispersal, gene flow among areas
77 that are well connected through larval transport can be limited by settlement regulation due to
78 space limitations (Roughgarden et al. 1985). However, the primary filter of connectivity is larval

79 transport, which is notably driven by the amount of time that larvae spend being transported by
80 ocean currents, otherwise known as the pelagic larval duration (PLD). Hence, the PLD has been
81 the primary factor considered in biophysical modeling when attempting to differentiate dispersal
82 distance capabilities among different species (Shanks et al. 2003).

83 Genetic studies have tested the relationship between realized connectivity (gene flow)
84 and the PLD following the same reasoning, and the results have led to contrasting conclusions
85 (Kinlan and Gaines 2003; Weersing and Toonen 2009; Riginos et al. 2011, D'Aloia et al. 2015).
86 Several arguments have been invoked to explain the absence of a relationship between PLD and
87 realized dispersal distance and migration rates, with some arguments referring to the way in
88 which realized connectivity is inferred from measures of genetic differentiation among
89 populations. For instance, the inverse relationship between the most common metric of genetic
90 differentiation, F_{ST} , and the migration rate (Wright's Island Model 1931), may be blurred by the
91 uncertainty of the estimation of the effective size of the population (Faurby and Barber 2012).
92 However, the failure to identify a relationship between PLD and realized connectivity is more
93 likely explained by the lack of unequivocal correlation between PLD and dispersal distance. In
94 fact, the variability of ocean currents (Cowen et al. 2006, Guizien et al. 2014), larval behavior
95 (Guizien et al. 2006, Paris et al. 2007) and larval mortality (Cowen et al. 2000) can lead to very
96 different dispersal patterns given the same PLD. Moreover, for any given species, PLD does not
97 have a single value, but it varies along a competency window (Arnold and Steneck 2011), within
98 which successful recruitment can occur at any time once a suitable habitat is found along the
99 dispersal pathway.

100 To determine which biological filters transform larval release into gene flow (potential
101 into realized connectivity), we used one of the most abundant and conspicuous species of the
102 rocky sublittoral zone in the northwestern Mediterranean Sea, the white gorgonian *Eunicella sin-*
103 *gularis*.

104 In the hydrodynamic province of the Gulf of Lion (NW Mediterranean, Rossi et al. 2014),

105 the spatial distribution of *E. singularis* is discontinuous (Gori et al. 2011) due to fragmentation of
106 the rocky habitat (Aloisi et al. 1973). *E. singularis* is believed to play an important ecological role
107 due to its erect structure, which provides habitat for the local epifauna and increases the biomass
108 and diversity of the rocky community (Ballesteros 2006; Mitchell et al. 1992). Furthermore, its
109 indirect economic value due to its contributions to shaping the seascape and attracting SCUBA
110 diving and fishing activities makes *E. singularis* a species of interest in the monitoring plans of
111 all MPAs in the Gulf of Lion. *E. singularis* is a long-lived (up to 15 years) internal brooding ses-
112 sile species. Lecitotrophic larvae (planulae) are released once a year in June-July (Théodor 1967;
113 Weinberg and Weinberg 1979). Larvae can survive up to 122 days in *ex situ* experiments in the
114 absence of predation (Théodor 1967), with 50% to 80% survival after 40 days (K. Guizien, *Per-*
115 *sonal communication*). Competency for recruitment was observed after a few days and lasted up
116 to a few weeks (L. Bramanti, *Personal communication*). Such larval traits suggest a wide disper-
117 sive potential of the species.

118 In the present study, we propose a methodological approach that combines demographic,
119 biophysical and genetic methods to test the relationship between the dispersive potential of a ses-
120 sile benthic species and the effective gene flow in a fragmented habitat layout. The study aims to
121 (1) assess the genetic structure of *Eunicella singularis* within the fragmented habitat of the Gulf
122 of Lion, (2) test the role of demographic filters (i.e., reproductive output and intra-specific recruit-
123 ment limitations) in shaping gene flow, and (3) test the significance of various PLD-driven larval
124 transport modes in shaping the spatial pattern of gene flow.

125

126 **MATERIAL AND METHODS**

127 **Study area and regional hydrodynamics**

128 The Gulf of Lion (hereafter GoL) is a large (~100 km), microtidal continental shelf with a
129 100-km radius located in the northwestern Mediterranean Sea (Figure 1). The first 30 meters of
130 the bathymetry is mainly covered by soft sandy sediment; however, fragmented patches of hard

131 substrate can be found in the eastern (Côte Bleue), central (Plateau des Aresquiers and Cap
132 d'Agde), and western (Cap Leucate and Côte Vermeille) parts of the gulf (Aloisi et al. 1973).
133 Circulation in the GoL is driven by three main forces: 1) strong continental winds from the north
134 (Mistral) and the northwest (Tramontane) that frequently generate upwelling and downwelling
135 along the coast, as well as transient currents and eddies; 2) the Northern Current (NC), which
136 usually flows westward along the shelf break of the GoL from the Ligurian Sea to the Catalan
137 Sea; 3) river inputs, particularly from the Rhône, that deliver freshwater and high nutrient and
138 organic matter loads (Millot 1990; Hu et al. 2009; Campbell et al. 2013).

139 Numerical simulations at the basin scale have identified that the GoL is an isolated
140 hydrodynamic province, with the Northern Current acting as a hydrodynamic barrier that limits
141 the transport of particles across the shelf break (Rossi et al. 2014). Large-scale flow limits entries
142 into the Gulf of Lion up to a 60-day PLD from the east and up to a 30-day PLD from the west.
143 Moreover, despite an overall westward drift leading to large sediment exports through western
144 canyons (Ulses et al. 2008), persistent anticyclonic eddies are observed in the southwestern part
145 of the GoL during the summer (Hu et al. 2009), and connectivity patterns within the Gulf of Lion
146 stabilize after 3 weeks.

147 **Sampling design**

148 From July 2013 to October 2014, detectable colonies (taller than 1 cm) of *Eunicella*
149 *singularis* were counted and sampled at 17 geo-referenced stations distributed along the GoL,
150 from the Côte Bleue to the Côte Vermeille (Table 1) (Figure 1). The stations were distributed
151 along four rocky habitat patches separated by large areas of sandy bottom (Côte Bleue, Plateau
152 des Aresquiers, Cap d'Agde and Côte Vermeille) at depths between 15 and 35 meters. The
153 distance between stations varied from less than 1 km to 180 km. The population size structures
154 were similar in the four rocky habitat patches, with 25% of the colonies smaller than 5 cm, 55%
155 of the colonies between 5 and 20 cm and 20% of the colonies taller than 20 cm (L. Bramanti,
156 *Personal communication*). The number of stations sampled in each habitat patch varied according

157 to the along-shore extension of *E. singularis* coverage of the rocky bottom (L. Bramanti,
158 *Personal communication*). In Côte Bleue, where the smallest coverage of *E. singularis* was
159 found, only three stations were sampled; in Plateau des Aresquiers and Cap d'Agde, four stations
160 were sampled, while six stations were sampled in the Côte Vermeille.

161 The mean population density at each station was calculated from colony counts in 4
162 quadrats (1 m² each). For each station, the 4 quadrats were located 5 m from the geo-referenced
163 station, one in each of the four cardinal directions. Small apical fragments (<3 cm) of all colonies
164 of *E. singularis* that were counted at each station were collected, preserved in 95% ethanol and
165 kept at 6 °C until DNA extraction. For the present study, 13 to 36 colonies per station were
166 randomly selected and genotyped, for a total of 434 colonies.

167 **Genetic diversity and population structure**

168 All colonies were genotyped at eight microsatellite loci specifically developed for *E.*
169 *singularis*: C21, C30 and C40 (Molecular Ecology Resources Primer Development Consortium
170 2010) and *E. verrucosa*: Ever003, Ever004, Ever009, Ever013 and Ever014 (Holland et al. 2013)
171 after DNA extraction (Appendix S1). The scoring of the alleles was carried out using
172 GeneMapper v.3.7 software (Applied Biosystems). We calculated the summary statistics of the
173 genetic diversity (allelic richness, observed heterozygosity, expected heterozygosity), and tested
174 for departure from the Hardy-Weinberg equilibrium, linkage disequilibrium and the presence of
175 null alleles (Appendix S1). The statistical power to detect the level of genetic variation among
176 populations was estimated using Powsim v.4.1 (Ryman and Palm 2006). The spatial genetic
177 structure of *E. singularis* was analyzed by testing for the presence of a pattern using the isolation
178 by distance (IBD) and the Loiselle kinship coefficient (Appendix S1). The patterns of population
179 genetic structure were analyzed using F_{ST}, a Bayesian clustering method that identifies clusters of
180 individuals who share similar patterns of variation (Structure v.2.3.4; Pritchard et al. 2000) and a
181 hierarchical analysis of molecular variance (AMOVA). For details, see the Methods in Appendix
182 S1.

183 **Contemporary gene flow**

184 The genotyped individuals from the 17 stations were clustered into 4 groups defined by
185 habitat discontinuity, corresponding to the four largest rocky habitat patches (Côte Vermeille,
186 Cap d'Agde, Plateau des Aresquiers and Côte Bleue). Contemporary gene flow over the last 2-3
187 generations was estimated in the form of matrices containing migration rates including a proxy of
188 self-recruitment among these 4 clusters using BayesAss 3.0 applied on multilocus genotypes
189 (Wilson and Rannala 2013). It is important to note that the BayesAss 3.0 output is the proportion
190 of individuals in the destination population that is descendant from a source population.

191 The confidence intervals and the uncertainty values around the average migration rates were
192 estimated (Appendix S1).

193 **Recent larval transport**

194 Using the 3D ocean model Symphonie (S-2010 release 26, at <http://sirocco2.omp.obs->
195 [mip.fr/outils/Symphonie/Accueil/SymphoAccueil.htm](http://sirocco2.omp.obs-mip.fr/outils/Symphonie/Accueil/SymphoAccueil.htm)), high-resolution flow simulations were
196 carried out and used for larval dispersal simulations (Appendix S1). The latter were upscaled to
197 the larval transport matrices for single reproductive events. Larval transport matrices contain
198 transfer rate values defined as the proportion of larvae (neutrally buoyant particles) released from
199 a source habitat patch (row) during a given release period that reach a destination habitat patch
200 (column) after a given PLD. Fifteen variations of larval transport matrices were established per
201 PLD, with each variant corresponding to a non-overlapping weeklong release period in June (five
202 variants per year) over three years (2010, 2011, 2012, Appendix S1). Six weeks of dispersal were
203 simulated and eight PLD values ranging from 3.5 to 42 days were tested. The PLD range that was
204 tested was greater than the period during which *Eunicella singularis* larvae competency for
205 recruitment as observed in laboratory experiments (L. Bramanti, *Personal Communication*).
206 Moreover, the maximum PLD tested in the present study (42 days) was longer than the time
207 required to observe stable connectivity patterns within the Gulf of Lion (Briton et al., submitted).

208 **Comparison between larval transport and gene flow**

209 With gene flow being estimated as the proportion of individuals in the destination
210 population that is a descendant from a source population, and larval transport being the
211 proportion of the larvae released from a source population that arrives in a destination population,
212 comparing gene flow and larval transport requires a series of data transformations (see details in
213 Appendix S1). Briefly, as the actual number of larvae released from a source population is
214 unknown, the transformation of larval transport into the number of larvae reaching a destination
215 population is not possible. Hence, gene flow was transformed into the proportion of migrants that
216 leaves a source population and arrives at each destination population. For each PLD, recent larval
217 transport was estimated as the average of the 15 larval transport matrix variants (one for each
218 single reproductive event). Recent larval transport matrices were normalized so that the sum of
219 the destination probabilities from the same source (i.e., all columns within each row) was equal to
220 one, which removed the proportion of larvae dispersed out of the 4 habitat patches sampled for
221 genetics as this proportion is not included in the gene flow assessment. It is worth noting that
222 after these normalizations, for both the gene flow and larval transport matrices, only rows, not
223 columns, are statistically independent. Hence, the significance of the Pearson product-moment
224 correlations (excluding diagonal terms, i.e., retention rates) between the contemporary gene flow
225 and recent larval transport matrices (4x4) was tested using a Mantel test (Mantel 1967) for all 24
226 possible permutations, after modifying the random QAP.m Matlab routine by Puck Rombach
227 (2011). In addition, the determination coefficient between contemporary gene flow and recent
228 larval transport was computed including diagonal terms, i.e., retention rates.

229 **Relationship between population density and migration**

230 Finally, the effect of demographic filters on the number of migrants (see calculation in
231 Appendix S1) was tested, namely, the modulation of emigrants by reproductive output from the
232 source populations and the modulation of immigrants by settlement limitation in the destination
233 populations. Two correlation analyses were performed to test the relationship between 1) the
234 number of contemporary emigrants from a source habitat patch (sum of migrants number by row)

235 and the mean population density in that source (proxy of reproductive output given the same
236 population size structure in all habitat patches), and 2) the number of contemporary immigrants to
237 a destination habitat patch (sum of migrant numbers by column) and the mean population density
238 in that destination patch (proxy of intra-specific competition). All statistical analyses were
239 conducted in Matlab (R2012a).

240

241 **RESULTS**

242 **Genetic diversity and population structure**

243 All sampled individuals were included in the analysis (no identical multilocus
244 genotypes). All loci were polymorphic, with more than 4 alleles among stations on average and
245 from 5 to 13 alleles over all loci, which is comparable to the degree of polymorphism obtained by
246 Holland et al. (2013). Linkage disequilibrium was not observed (Appendix S2, Table A2). The
247 observed and expected heterozygosities were similar among stations with no significant
248 heterozygote excesses, but there were significant heterozygote deficits across two populations
249 (CV1 and CA1) (Appendix S2, Table A2) and in two of the eight loci (Ever003 and C40)
250 (Appendix S2, Table A3). The frequency of null alleles was negligible (Appendix S2, Table A3).

251 The overall F_{ST} value was low (0.04), and almost all pairwise F_{ST} values among stations
252 were significantly different (P-value < 0.001) (Appendix S2, Table A4). Nei's genetic distance
253 values were closer among the stations within habitat patches than between them (Figure 2). While
254 the stations in Côte Bleue and Cap d'Agde-Plateau des Aresquiers are close to each other, the
255 stations in the Côte Vermeille (CV) appear more scattered along the first axis, with one station
256 (CV5) falling near the stations of Cap d'Agde and Plateau des Aresquiers (CA and PA,
257 respectively).

258 The Bayesian clustering analysis identified three genetic clusters ($K = 3$) (mean $\ln P(K) =$
259 -7532.99 ; $\Delta K = 25.09$). The resulting clustering partially corresponded to the rocky habitat
260 fragmentation in the region (Figure 3): Côte Vermeille (6 stations), Cap d'Agde and Plateau des

261 Aresquiers (8 stations), and Côte Bleue (3 stations). Some individuals in Côte Vermeille depicted
262 higher similarity to individuals from Cap d'Agde and Plateau des Aresquiers rather than to other
263 individuals in Côte Vermeille. The results of the AMOVA confirmed the clustering structure ($P <$
264 0.001) (Appendix S2, Table A5).

265 The correlation between $F_{ST} / (1-F_{ST})$ and the logarithm of the geographic distance ($R^2 =$
266 0.28 ; P -value = 0.01) was significant but low among the 17 stations in the GoL and was not
267 significant among the 4 patches defined according to rocky habitat fragmentation ($R^2 = 0.81$; P -
268 value = 0.100) (Appendix S2, Figure A2). The estimated maximum size of the genetic patch
269 based on Loiselle's kinship coefficient was 30 km, which is larger than the maximum size of any
270 of the habitat patches in the Gulf of Lion (Appendix S2, Figure A3).

271 **Contemporary gene flow**

272 Figure 4 shows the spatial patterns of the number of contemporary migrants among the 4
273 separated habitat patches in the GoL. The uncertainty of the migration pattern, following an error
274 metric adapted from the Euclidean matrix norm (see details in Appendix S1), was below 25%.

275 Local retention dominated over emigration in all habitat patches. However, local retention was
276 much lower in Côte Bleue (mean = 51 migrants, CI (95%) = 48 – 52 migrants) compared to all
277 other habitat patches (from 90 to 121 migrants) and was comparable to the value of emigration
278 from Cap d'Agde (45 ± 14 migrants). Cap d'Agde acted as a hub, distributing migrants to both
279 Côte Vermeille (westward) (mean = 16 migrants, CI (95%) = 6-19 migrants) and Plateau des
280 Aresquiers (eastward) (mean = 28 migrants, CI (95%) = 17-34 migrants).

281 **Relationship between population density and migration**

282 Neither the number of contemporary emigrants coming from a habitat patch (Figure 5A)
283 nor the number of contemporary immigrants arriving to a habitat patch (Figure 5B) showed a
284 significant correlation with the population density of the source ($R^2 = 0.203$, $P > 0.05$) or the
285 destination ($R^2 = 0.787$, $P > 0.05$) habitat patch, respectively.

286 Although the lowest number of emigrants corresponded to the source habitat patch with
287 the lowest population density, the opposite was not true. The highest number of emigrants did not
288 come from the habitat patch with the highest population density. The number of immigrants did
289 not decay with increasing population density in the destination habitat patch but conversely
290 increased. However, a similar number of immigrants were found in the destination habitat patches
291 with quite different population densities.

292 **Comparison between recent larval transport and contemporary gene flow**

293 In the following section, both larval transport and gene flow have been normalized for
294 each source population and are subsequently no longer comparable between different source
295 populations. Recent larval transport varied greatly among the PLDs ranging from 3.5 to 42 days:
296 from a scenario of high local retention within all habitat patches to a scenario of high levels of
297 larval transport among most habitat patches, except Côte Vermeille (Figure 6A to 6E). Larval
298 transport was restricted to the exchange between Cap d'Agde and Plateau des Aresquiers for the
299 shortest PLD tested (3.5 days, Figure 6A), and increased in a westward direction for the PLDs
300 longer than 14 days (Figures 6D, 6E and data not shown). For the PLDs of 7 and 10.5 days
301 (Figure 6B and 6C), larval transport was westward from Plateau des Aresquiers and Côte Bleue,
302 but both westward and eastward from Cap d'Agde. Moreover, it is interesting to note that the
303 local retention decayed more rapidly in Cap d'Agde compared to the other habitat patches due to
304 efficient larval export towards the closest habitat patches of Plateau des Aresquiers and Côte
305 Vermeille. This pattern matched the one observed for contemporary gene flow particularly well
306 (Figure 6F).

307 The Mantel test showed a significant correlation (Mantel statistics <5%) between
308 contemporary gene flow and recent larval transport (excluding retention rates) only for the PLDs
309 ranging from 7 to 14 days with a determination coefficient (including retention rates) larger than
310 50% (Figure 7). However, the determination coefficient between contemporary gene flow and
311 recent larval transport, which includes retention rates, was also high for a PLD of 3.5 days (R^2

312 >0.95). Interestingly, the determination coefficient did not decrease monotonically with PLD but
313 rather peaked at a PLD of 7 days ($R^2 = 0.98$).

314

315 **DISCUSSION**

316 *Habitat fragmentation fails to explain regional genetic structure of Eunicella singularis in the*
317 *Gulf of Lion*

318 The analysis of the genetic differentiation of groups of *Eunicella singularis* colonies
319 among a wide range of spatial scales (from less than 1 km to 180 km) showed high levels of
320 genetic variability at small scales with a deficit of heterozygotes at some stations, as reported
321 previously for the same species (Costantini et al. 2016) and in other Mediterranean gorgonians
322 such as *Paramuricea clavata* (Mokhtar-Jamaï et al. 2011) and *Corallium rubrum* (Costantini et
323 al. 2007). In these studies, genetic patchiness was attributed to inbreeding, putatively due to the
324 low dispersal ability of the larvae. However, the genetic clustering analysis of *E. singularis*
325 populations in the GoL revealed strong similarity among the individuals sampled in Cap d'Agde
326 and Plateau des Aresquiers, which are separated by 30 km of sandy bottom that is unsuitable for
327 colonization by the species (Weinberg 1978). Moreover, one station in the Côte Vermeille cluster
328 displayed higher similarity to the stations at Cap d'Agde and Plateau des Aresquiers than to the
329 other stations in Côte Vermeille. These similarities to the genetic profiles of distant stations led to
330 an estimated genetic patch size of 30 km, meaning that the individuals found within an area of 30
331 km would be more genetically related than those taken randomly from any further distance. These
332 results, together with the absence of genetic structure among *E. singularis* populations found
333 within 15 km (Costantini et al. 2016) in the neighboring hydrodynamic province (Balearic Sea,
334 Rossi et al. 2014), suggest that the heterozygote deficit in the *E. singularis* populations in the
335 GoL should be attributed to on-going migration among open populations rather than to inbreeding
336 in closed populations. Nevertheless, migration was not explained by isolation by distance (Sexton
337 et al. 2013; Nanninga et al. 2014; Thomas et al. 2015), which pinpoints the limitation of using the

338 IBD model to explain the chaotic genetic patchiness resulting from larval dispersal via ocean flow
339 (Selkoe et al. 2010). Indeed, undirected pairwise F_{ST} is not a good measure of genetic distance
340 when migration among populations is asymmetrical (Beerli 1998; Broquet and Petit 2004; van
341 Strien et al. 2015). In such a case, assignment tests or coalescent methods should be used to
342 describe gene flow patterns and determine the factors shaping them (Manel et al. 2005).

343 *Gene flow is determined by larval transport*

344 We tested three major successive filters that potentially influence gene flow during larval
345 dispersal among habitat patches. First, the number of emigrants of *E. singularis* within separated
346 habitat patches in the GoL was not explained by reproductive output. Second, the number of
347 immigrants was not limited by settlement regulation due to intra-specific competition, although
348 this mechanism is often presented (Roughgarden et al., 1985; Padron and Guizien 2015). It is
349 interesting to note that conversely, the population density in the destination habitat patch
350 increased with the number of immigrants, suggesting that the population densities observed in the
351 GoL were below habitat saturating capacity. Third, larval transport explained a large portion of
352 the gene flow among populations. In the GoL, the determination coefficient between
353 contemporary gene flow and recent larval flow was extremely high for a 7-day larval transport
354 duration among four habitat patches.

355 The combination of the absence of a density-dependent regulation of *E. singularis* migrants in the
356 GoL and the fact that gene flow is driven by unsteady larval transport support the alternate
357 dominance of recruits vs. adult colony populations hypothesis that was observed for the same
358 species along the Costa Brava (NW Mediterranean, Spain) (Linares et al. 2008). The strong
359 correlation between recent larval transport and contemporary gene flow found in this study
360 contrast with other studies based on the correlation with multi-generational gene flow (White et
361 al. 2010; Alberto et al. 2011). This underpins the importance of testing the relationship between
362 larval transport and gene flow estimated for a single dispersive event rather than for multiple

363 generations. Moreover, estimations at the single dispersive event scale enabled the discrimination
364 of the efficiency of different PLDs in connecting populations.

365 *The environment filters the PLDs that connect populations*

366 *Ex situ* observations of survival expectancy and competency duration of *E. singularis*
367 larvae (up to 40 days, K. Guizien and L. Bramanti, *Personal Communication*) suggest that all
368 tested PLDs were equally probable in the absence of predation. In such a case, one would expect
369 gene flow to be a composite of larval transport for all PLDs. However, gene flow among
370 populations was best explained by PLDs ranging from 7 to 14 days in the habitat configuration of
371 the GoL, and led to a spatially structured genetic population despite high local chaotic genetic
372 patchiness. Similar finding was obtained among lobster populations along the Californian coast
373 and related to upwelling intensity (Iacchei et al. 2013). In the present case of a lecithotrophic
374 larva with a wide competence window, we suggest that larval mortality significantly altered larval
375 transport patterns for periods longer than 14 days (Cowen et al. 2000). Correlatively, it suggests
376 that mortality, particularly by predation, on *Eunicella singularis* larvae (2-3 mm) can be
377 neglected up to a 14-day PLD in the GoL.

378 Trembl et al. (2012) found that longer maximum PLDs lead to a more connected seascape
379 on an ocean basin scale. The study claimed that maximum PLD is a good predictor of larval
380 transport at large geographic scales (200-500 km) but a poor predictor at a mesoscale (<200 km).
381 Our study evaluated the larval transport patterns among populations at a regional scale (up to 180
382 km) and showed that the PLD-indexed larval transport could significantly determine gene flow at
383 a mesoscale. Our findings suggest that several PLDs should be tested along the competency
384 period of a species rather than the average or the maximum PLD to provide a more accurate
385 assessment of the importance of larval transport in shaping gene flow among sessile benthic
386 species (D'Aloia et al. 2015).

387 *Implications for conservation*

388 Our results have important implications for regional conservation and the spatial

389 management of benthic sessile species in the GoL. Empirical gene flow patterns allow for the
390 identification of key habitat patches of *E. singularis*: the high levels of gene flow between Cap
391 d'Agde and Plateau des Aresquiers, along with transfers to other habitat patches, suggest that
392 these two areas play a pivotal role in the spread of *E. singularis* in the region. Furthermore, the
393 significant correlation between contemporary gene flow and recent larval transport for a PLD
394 ranging from 7 to 14 days suggests that Cap d'Agde and Plateau des Aresquiers could be
395 important sites for any species with similar dispersive traits (PLD, larval behavior, or
396 reproductive period) dwelling on the same rocky substrate, as they should follow the same
397 potential connectivity patterns. Hence, we advocate for enforcing the protection of those sites
398 already identified as important for the regional persistence of soft-bottom species (Guizien et al.
399 2014), which also appears to be functionally important for the life cycle of some rocky species.

400 In summary, the methodological approach presented in this study highlights the hidden
401 determinism within the apparent genetic chaos by incorporating interdisciplinary data
402 (demography and ocean currents) and applying accurate genetic tools (coalescent-based analyses)
403 to evaluate the gene flow among populations.

404

405 **Authors' Contributions**

406 M.P., L.B., and K.G. designed the study. S.B. performed all the laboratory work. M.P., F.C. and
407 K.G. analyzed all the data. All authors contributed to the writing of the manuscript.

408

409 **Data Accessibility**

410 Microsatellite genotypes will be made available in Dryad.

411

412 **Acknowledgements**

413 This work was (co-) funded through a MARES Grant. MARES is a Joint Doctorate program se-
414 lected under Erasmus Mundus coordinated by Ghent University (FPA 2011-0016). Check [www.-](#)

415 mares-eu.org for additional information. This work was also partially funded by the French Na-
416 tional Program LITEAU IV of the Ministère de l'Écologie et de l'Environnement Durable under
417 project RocConnect—Connectivité des habitats rocheux fragmentés du Golfe du Lion (PI, K.
418 Guizien, Project Number 12-MUTS-LITEAU-1-CDS-013. The authors particularly thank the sci-
419 entific managers of the Gulf of Lion MPA: S. Blouet, E. Charbonnel, B. Ferrari and J. Payrot for
420 valuable interactions during the study design. The authors gratefully acknowledge the helpful as-
421 sistance during sampling of R. Bricout, F. Cornette, S. Fanfard, B. Hesse, C. Labrune, L. Lescure,
422 J.-C. Roca, P. Romans, and the staff of the Réserve Naturelle Marine de Cerbère-Banyuls, Aire
423 Marine Protégée Agatoise, Parc Naturel Marin du Golfe du Lion and Parc Marin de la Côte
424 Bleue. We also acknowledge American Journal Experts for English editing service.

425

426 **REFERENCES**

427 Alberto F, Raimondi P, Reed D, Watson J, Siegel D, Mitarai S, Coelho N, Serrão E (2011) Isola-
428 tion by oceanographic distance explains genetic structure for *Macrocystis pyrifera* in the
429 Santa Barbara Channel. *Molecular Ecology* 20:2543–2554.

430 Aloisi J, Got H, Monaco A (1973) Carte géologique du précontinent languedocien au
431 1/250000ième. Enschede: International Institute for Aerial Survey and Earth Sciences,
432 Netherlands.

433 Arnold SN, Steneck R (2011) Setting into an increasingly hostile world: the rapidly closing “re-
434 cruitment window” for corals. *PLoS ONE* 6:e28681.

435 Ballesteros E (2006) Mediterranean coralligenous assemblages: a synthesis of present knowledge.
436 *Oceanography and Marine Biology* 44:1–74.

437 Beerli P (1998) Estimation of migration rates and population sizes in geographically structured
438 populations. In: Carvalho G. (eds) *Advances in Molecular Ecology* (NATO Science Series
439 A: Life Sciences, Vol. 306). IOS Press, Amsterdam, pp 39–53.

440 Beerli P, Felsenstein J (2001) Maximum likelihood estimation of a migration matrix and effec-
441 tive population sizes in n subpopulations by using a coalescent approach. *Proceedings of the*
442 *National Academy of Sciences* 98:4563–4568.

443 Broquet T, Petit E (2004) Quantifying genotyping errors in noninvasive population genetics.
444 *Molecular Ecology* 13:3601–3608.

445 Campbell R, Diaz F, Hu Z, Doglioli A, Petrenko A, Dekeyser I (2013) Nutrients and plankton
446 spatial distributions induced by coastal eddy in the Gulf of Lion. *Insights from a numerical*

- 447 model. Progress in Oceanography 109:47–69.
- 448 Costantini F, Fauvelot C, Abbiati M (2007) Genetic structuring of the temperate gorgonian coral
449 (*Corallium rubrum*) across the western Mediterranean Sea revealed by microsatellites and
450 nuclear sequences. Molecular Ecology 16:5168–5182.
- 451 Costantini F, Gori A, López-González P, Bramanti L, Rossi S, Gili J-M, Abbiati M (2016) Lim-
452 ited genetic connectivity between gorgonian morphotypes along a depth gradient. PLoS ONE
453 11:e0160678.
- 454 Cowen R (2000) Connectivity of marine populations: open or closed? Science 287:857–859.
- 455 Cowen R (2006) Scaling of connectivity in marine populations. Science 311:522–527.
- 456 D’Aloia C, Bogdanowicz S, Francis R, Majoris J, Harrison R, Buston P (2015) Patterns, causes,
457 and consequences of marine larval dispersal. Proceedings of the National Academy of Sci-
458 ences 112:13940–13945.
- 459 Dawson M, Hays C, Grosberg R, Raimondi P (2014) Dispersal potential and population genetic
460 structure in the marine intertidal of the eastern North Pacific. Ecological Monographs
461 84:435–456.
- 462 Faurby S, Barber P (2012) Theoretical limits to the correlation between pelagic larval duration
463 and population genetic structure. Molecular Ecology 21:3419–3432.
- 464 Gori A, Rossi S, Berganzo E, Pretus J, Dale M, Gili JM (2011) Spatial distribution patterns of the
465 gorgonians *Eunicella singularis*, *Paramuricea clavata*, and *Leptogorgia sarmentosa* (Cape
466 of Creus, Northwestern Mediterranean Sea). Marine Biology 158:143–158.
- 467 Guizien K, Brochier T, Duchêne JC, Koh BS, Marsaleix P (2006) Dispersal of *Owenia fusiformis*

468 larvae by wind-driven currents: turbulence, swimming behaviour and mortality in a three-di-
469 mensional stochastic model. *Marine Ecology Progress Series* 311:47–66.

470 Guizien K, Belharet M, Moritz C, Guarini JM (2014) Vulnerability of marine benthic metapopu-
471 lations: implications of spatially structured connectivity for conservation practice in the Gulf
472 of Lions (NW Mediterranean Sea). *Diversity and Distributions* 1–11.

473 Hanski I (1998) Metapopulation dynamics. *Nature* 396:41–49.

474 Holland L, Dawson D, Horsburgh G, Krupa A, Stevens J (2013) Isolation and characterization of
475 fourteen microsatellite loci from the endangered octocoral *Eunicella verrucosa* (Pallas 1766).
476 *Conservation Genet Resour* 5:825–829.

477 Hu ZY, Doglioli AM, Petrenko AA, Marsaleix P, Dekeyser I (2009) Numerical simulations of
478 eddies in the Gulf of Lion. *Ocean Modelling* 28:203–208.

479 Iacchei M, Ben-Horin T, Selkoe KA, Bird CE, Garcia-Rodrigues FJ, Toonen RJ (2013) Com-
480 bined analyses of kinship and FST suggest potential drivers of chaotic genetic patchiness in
481 high gene-flow populations. *Mol Ecol* 22:3476–3494.

482 Kinlan B, Gaines S (2003) Propagule dispersal in marine and terrestrial environments: a commu-
483 nity perspective. *Ecology* 84:2007–2020.

484 Liggins L, Treml E, Riginos C (2013) Taking the plunge: an introduction to undertaking seascape
485 genetic studies and using biophysical models. *Geography Compass* 7:173–196.

486 Linares C, Coma R, Garrabou J, Diaz D, Zabala M (2008) Size distribution, density and distur-
487 bance in two Mediterranean gorgonians: *Paramuricea clavata* and *Eunicella singularis*.
488 *Journal of Applied Ecology* 45:688–699.

- 489 Manderson J (2016) Seascapes are not landscapes: an analysis performed using Bernhard Rie-
490 mann's rules. ICES J. Mar. Sci. 73:1831–1838.
- 491 Manel S, Gaggiotti O, Waples R (2005) Assignment methods: matching biological questions with
492 appropriate techniques. Trends in Ecology & Evolution 20:136–142.
- 493 Mantel N (1967) The Detection of Disease Clustering and a Generalized Regression Approach.
494 Cancer research 27(2) :209 -220
- 495 Millot C (1990) The Gulf of Lions' hydrodynamics. Continental shelf research 10:885–894.
- 496 Mitchell N, Dardeau M, Schaeffer W, Benke A (1992) Secondary production of gorgonian corals
497 in the northern Gulf of Mexico. Marine Ecology Progress Series 87:275–281.
- 498 Mokhtar-Jamaï K, Pascual M, Ledoux JB, Coma R, Féral JP, Garrabou J, Aurelle D (2011) From
499 global to local genetic structuring in the red gorgonian *Paramuricea clavata*: the interplay
500 between oceanographic conditions and limited larval dispersal. Molecular Ecology 20:3291–
501 3305.
- 502 Molecular Ecology Resources Primer Development Consortium (2010) Permanent genetic re-
503 sources added to molecular ecology resources database 1 August 2009 - 30 September 2009.
504 Molecular Ecology Resources 10:232–236.
- 505 Nanninga G, Saenz-Agudelo P, Manica A, Berumen ML (2014) Environmental gradients predict
506 the genetic population structure of a coral reef fish in the Red Sea. Molecular Ecology
507 23:591–602.
- 508 Padrón M, Guizien K (2015) Modelling the effect of demographic traits and connectivity on the
509 genetic structuration of marine metapopulations of sedentary benthic invertebrates. ICES

510 Journal of Marine Science. doi: 10.1093/icesjms/fsv158.

511 Paris C, Cherubin L, Cowen R (2007) Surfing, spinning, or diving from reef to reef: effects on
512 population connectivity. *Marine Ecology Progress Series* 347:285–300.

513 Pineda J, Hare J, Sponaugle S (2007) Larval transport and dispersal in the coastal ocean and con-
514 sequences for population connectivity. *Oceanologica Acta* 20:22–39.

515 Pritchard J, Stephens M, Donnelly P (2000) Inference of population structure using multilocus
516 genotype data. *Genetics* 155:945–959.

517 Riginos C, Douglas K, Jin Y, Shanahan D, Treml E (2011) Effects of geography and life history
518 traits on genetic differentiation in benthic marine fishes. *Ecography* 34:566–575.

519 Roberts C (1997) Connectivity and management of Caribbean coral reefs. *Science* 278:1454–
520 1457.

521 Rossi V, Ser-Giacomi E, López C, Hernandez-García E (2014) Hydrodynamic provinces and
522 oceanic connectivity from a transport network help designing marine reserves. *Geophysical*
523 *Research Letter* 41:2883–2891.

524 Roughgarden J, Iwasa Y, Baxter C (1985) Demographic theory for an open marine population
525 with space-limited recruitment. *Ecology* 66:54–67.

526 Ryman N, Palm S (2006) POWSIM: a computer program for assessing statistical power when
527 testing for genetic differentiation. *Molecular Ecology* 6:600–602.

528 Selkoe K, Watson J, White C, Horin T, Iacchei M, Mitarai S, Siegel D, Gaines S, Toonen R
529 (2010) Taking the chaos out of genetic patchiness: seascape genetics reveals ecological and
530 oceanographic drivers of genetic patterns in three temperate reef species. *Molecular Ecology*

- 531 19:3708–3726.
- 532 Selkoe K, D’Aloia C, Crandall E, Iacchei M, Liggins L, Puritz J, Heyden von der S, Toonen R
533 (2016) A decade of seascape genetics: contributions to basic and applied marine connectiv-
534 ity. *Marine Ecology Progress Series* 554:1–19.
- 535 Sexton J, Hangartner S, Hoffmann A (2013) Genetic isolation by environment or distance: which
536 pattern of gene flow is most common? *Evolution* 68:1–15.
- 537 Shanks A, Grantham B, Carr M (2003) Propagule dispersal distance and the size and spacing of
538 marine reserves. *Ecological Applications* 13:159–169.
- 539 Théodor J (1967) Contribution à l’étude des gorgones. VII. Ecologie et comportement de la plan-
540 ula. *Vie Milleu* 18:291–301.
- 541 Thomas L, Kennington W, Stat M, Wilkinson S, Kool J, Kendrick G (2015) Isolation by resis-
542 tance across a complex coral reef seascape. *Proceedings of the Royal Society B: Biological*
543 *Sciences* 282:20151217.
- 544 Treml E, Roberts J, Chao Y, Halpin P, Possingham H, Riginos C (2012) Reproductive output and
545 duration of the pelagic larval stage determine seascape-wide connectivity of marine popula-
546 tions. *Integrative and Comparative Biology* 52:525–537.
- 547 Ulses C, Estournel C, Durrieu de Madron X, Palanques A (2008) Suspended sediment transport
548 in the Gulf of Lions (NW Mediterranean): Impact of extreme storms and floods. *Continental*
549 *shelf research* 28:2048–2070.
- 550 van Strien MJ, Holderegger R, Van Heck HJ (2015) Isolation-by-distance in landscapes: consid-
551 erations for landscape genetics. *114:27–37.*

- 552 Weersing K, Toonen R (2009) Population genetics, larval dispersal, and connectivity in marine
553 systems. *Marine Ecology Progress Series* 393:1–12.
- 554 Weinberg S (1978) Mediterranean octocorallian communities and the abiotic environment. *Ma-
555 rine Biology* 49:41–57.
- 556 Weinberg S, Weinberg F (1979) The life cycle of a gorgonian: *Eunicella singularis*. *Bijdragen tot
557 de Dierkunde* 48:1–14.
- 558 White C, Selkoe K, Watson J, Siegel D, Zacherl D, Toonen R (2010) Ocean currents help explain
559 population genetic structure. *Proceedings of the Royal Society B: Biological Sciences*
560 277:1685–1694.
- 561 Wilson G, Rannala B (2003) Bayesian inference of recent migration rates using multilocus geno-
562 types. *Genetics* 163:1177–1191.
- 563 Wright S (1931) Evolution in Mendelian populations. *Genetics* 16:97–159.

564 **Figure 1.-** Locations of sampling stations and habitat patches of *Eunicella singularis* in the Gulf
565 of Lion, NW Mediterranean. A) Black rectangles highlight the sampled habitat patches. Red areas
566 show the distribution of the rocky habitat in the region. B) Sampling stations of *E. singularis* and
567 rocky habitat extent in the Côte Bleue. C) Sampling stations of *E. singularis* and rocky habitat
568 extent in the Côte Vermeille. D) Sampling stations of *E. singularis* and rocky habitat extent in
569 Cap d'Agde and Plateau des Aresquiers. Red squares correspond to the areas of larval release
570 considered in the hydrological model. Sampling stations are represented by gray dots.
571 Information for each station is provided in Table 1.

572

573 **Figure 2.-** Plot of the Principal Coordinate Analysis (PCoA) from the genetic distance matrix
574 assessed with pairwise Nei's genetic distance estimates of *E. singularis* in the Gulf of Lion. The
575 first two axes explain 61.51% of the variation.

576

577 **Figure 3.-** Population structure of *E. singularis* in the Gulf of Lion, as revealed by Structure
578 software. Each individual is represented by a vertical color line, with each color representing the
579 proportion of membership to each cluster. Black lines represent the division among the identified
580 clusters (K = 3). Values between parentheses correspond to the overall proportion of membership
581 of the individuals in each cluster.

582

583 **Figure 4.-** Patterns of contemporary migration among habitat patches of *Eunicella singularis* in
584 the Gulf of Lion. The matrix shows the number of migrants coming from any potential source and
585 reaching any destination habitat patch. CV = Côte Vermeille, CA = Cap d'Agde, PA = Plateau
586 des Aresquiers, and CB = Côte Bleue. The number of migrants between any two habitat patches
587 is represented by the grayscale intensity.

588

589 **Figure 5.-** A) Relationship between the number of emigrants (sum of number of migrants by row)
590 from a source habitat patch and the population density in that source habitat patch. B)
591 Relationship between the number of immigrants (sum of number of migrants by column) to a
592 destination habitat patch and the population density in that destination habitat patch. X error bars
593 correspond to the standard deviation around the mean population density values. Y error bars
594 correspond to the confidence intervals around the number of migrants estimated by BayesAss.

595

596 **Figure 6.-** Patterns of recent larval transport and contemporary gene flow among habitat patches
597 of *E. singularis* in the Gulf of Lion. A) Recent larval transport for a PLD of 3.5 days; B) recent
598 larval transport for a PLD of 7 days; C) recent larval transport for a PLD of 10.5 days; D) recent
599 larval transport for a PLD of 14 days; E) recent larval transport for a PLD of 21 days; F)
600 contemporary gene flow. The Grayscale indicates the probability values.

601

602 **Figure 7.-** Determination coefficient between contemporary gene flow and recent larval transport
603 (including retention rates) for a PLD ranging from 3.5 to 42 days. Filled circles depict the PLDs
604 for which the Mantel test showed significant correlations between contemporary gene flow and
605 recent larval transport matrices, excluding retention rates.

606

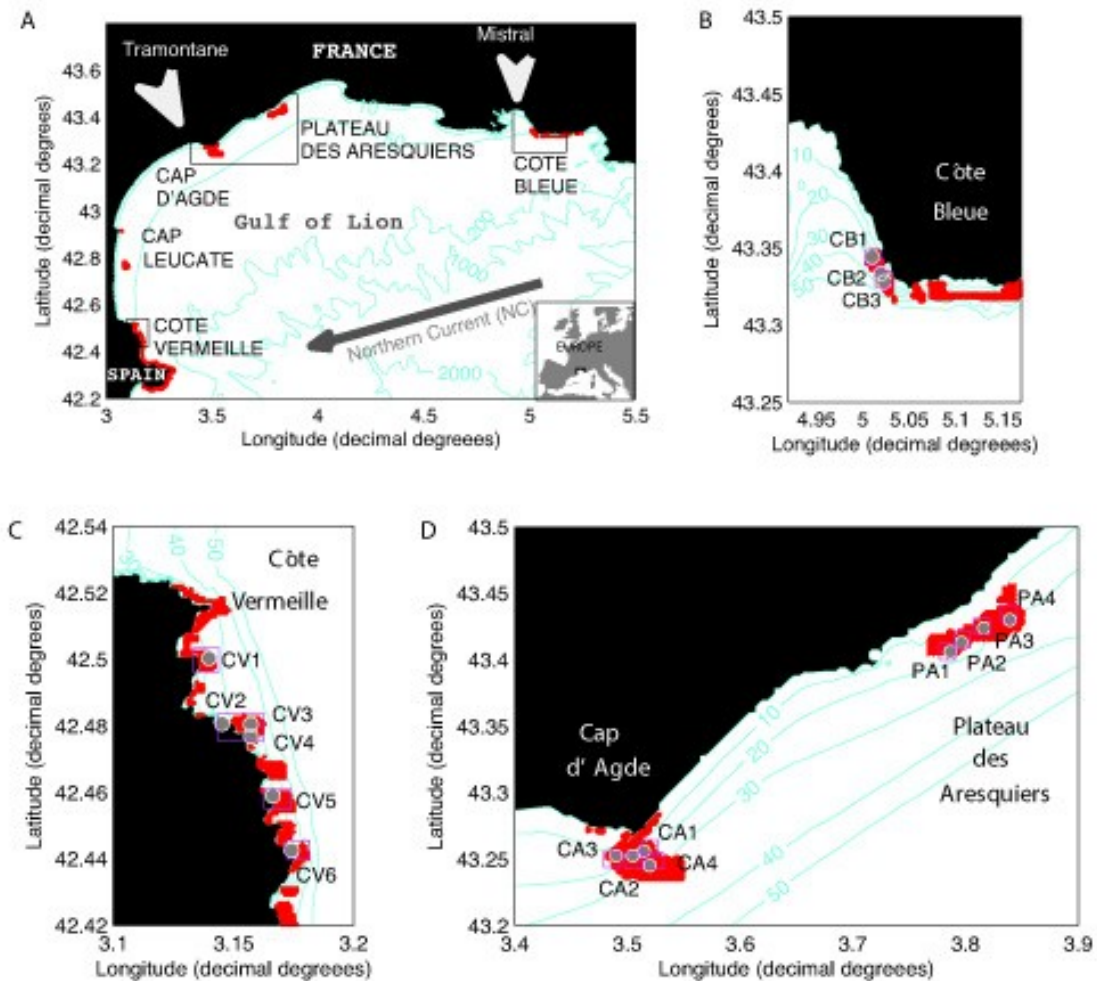


Figure 1.-Locations of sampling stations and habitat patches of *Eunicella singularis* in the Gulf of Lion, NW Mediterranean. A) Black rectangles highlight the sampled habitat patches. Red areas show the distribution of the rocky habitat in the region. B) Sampling stations of *E. singularis* and rocky habitat extent in the Côte Bleue. C) Sampling stations of *E. singularis* and rocky habitat extent in the Côte Vermeille. D) Sampling stations of *E. singularis* and rocky habitat extent in Cap d'Agde and Plateau des Aresquiers. Red squares correspond to the areas of larval release considered in the hydrological model. Sampling stations are represented by gray dots. Information for each station is provided in Table 1.

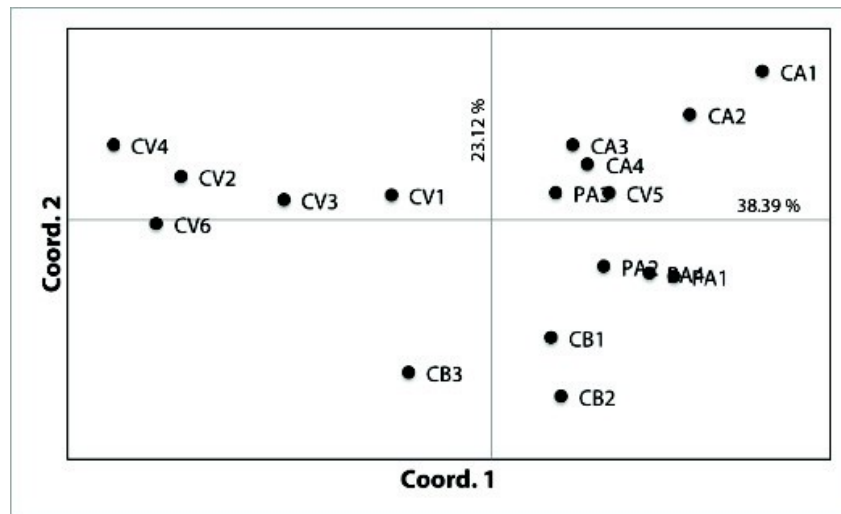


Figure 2.- Plot of the Principal Coordinate Analysis (PCoA) from the genetic distance matrix assessed with pairwise Nei's genetic distance estimates of *E. singularis* in the Gulf of Lion. The first two axes explain 61.51% of the variation.

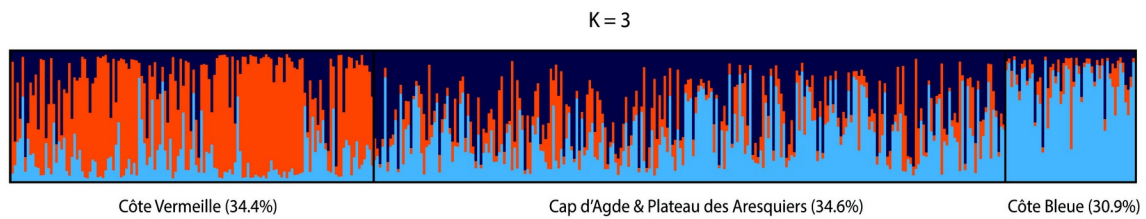


Figure 3.- Population structure of *E. singularis* in the Gulf of Lion, as revealed by Structure software. Each individual is represented by a vertical color line, with each color representing the proportion of membership to each cluster. Black lines represent the division among the identified clusters ($K = 3$). Values between parentheses correspond to the overall proportion of membership of the individuals in each cluster.

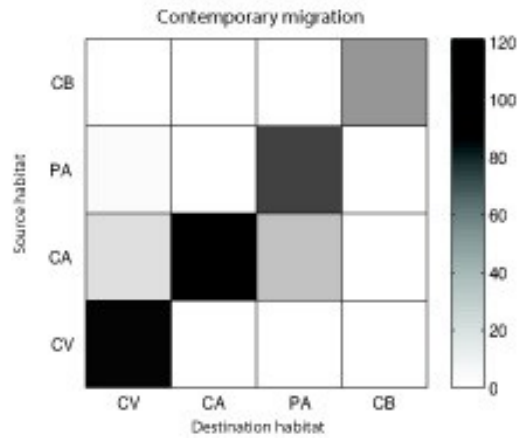


Figure 4.- Patterns of contemporary migration among habitat patches of *Eunicella singularis* in the Gulf of Lion. The matrix shows the number of migrants coming from any potential source and reaching any destination habitat patch. CV = Côte Vermeille, CA = Cap d'Agde, PA = Plateau des Aresquiers, and CB = Côte Bleue. The number of migrants between any two habitat patches is represented by the grayscale intensity.

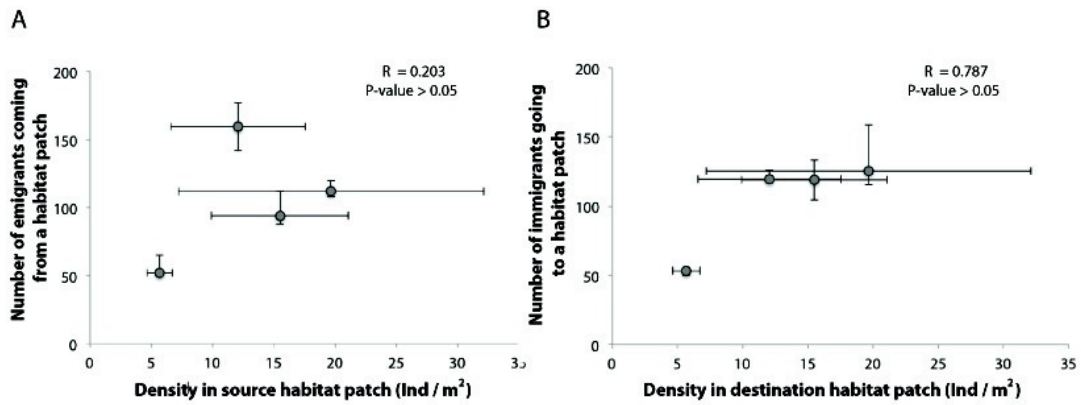


Figure 5.- A) Relationship between the number of emigrants (sum of number of migrants by row) from a source habitat patch and the population density in that source habitat patch. B) Relationship between the number of immigrants (sum of number of migrants by column) to a destination habitat patch and the population density in that destination habitat patch. X error bars correspond to the standard deviation around the mean population density values. Y error bars correspond to the confidence intervals around the number of migrants estimated by BayesAss.

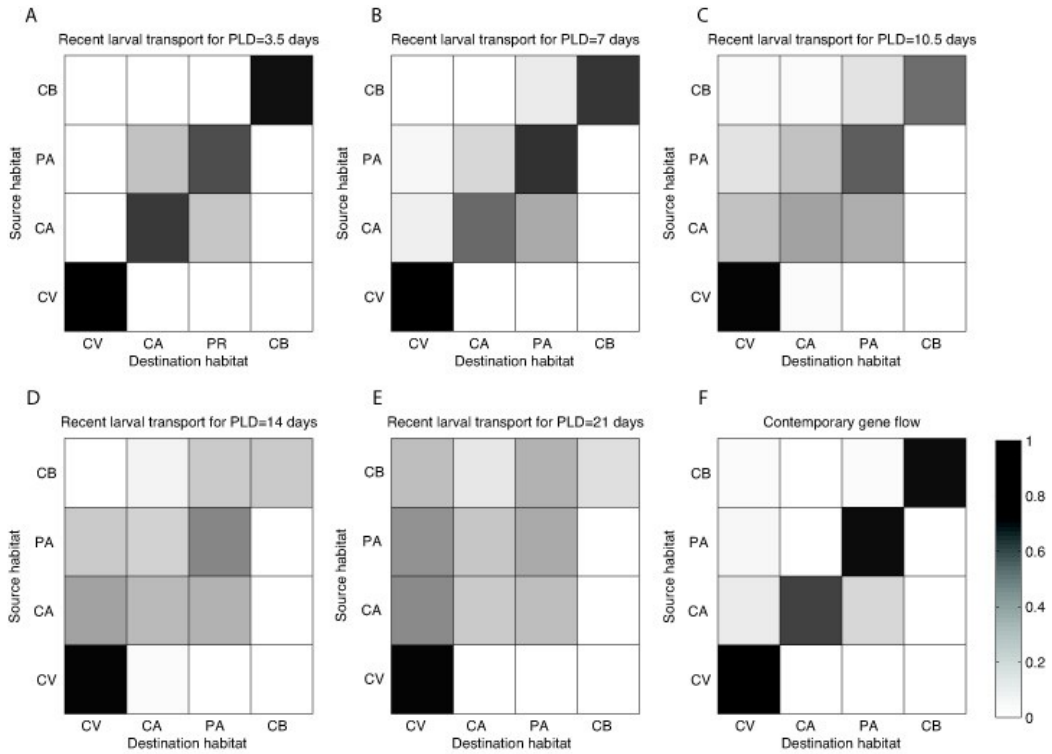


Figure 6.- Patterns of recent larval transport and contemporary gene flow among habitat patches of *E. singularis* in the Gulf of Lion. A) Recent larval transport for a PLD of 3.5 days; B) recent larval transport for a PLD of 7 days; C) recent larval transport for a PLD of 10.5 days; D) recent larval transport for a PLD of 14 days; E) recent larval transport for a PLD of 21 days; F) contemporary gene flow. The Grayscale indicates the probability values.

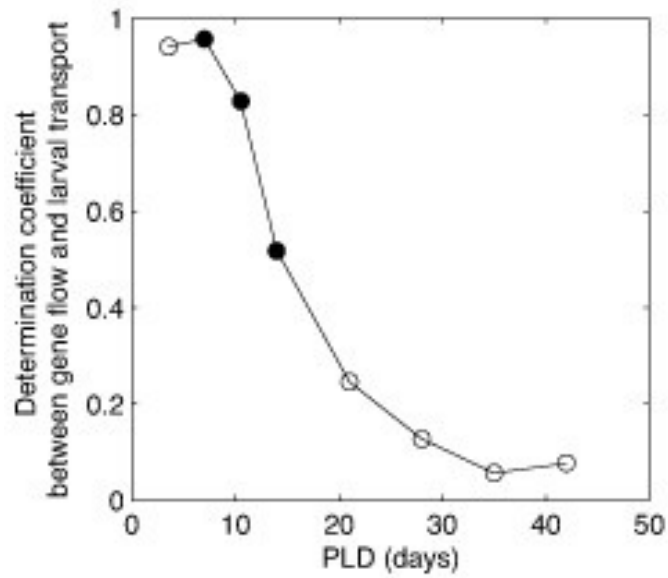


Figure 7.- Determination coefficient between contemporary gene flow and recent larval transport (including retention rates) for a PLD ranging from 3.5 to 42 days. Filled circles depict the PLDs for which the Mantel test showed significant correlations between contemporary gene flow and recent larval transport matrices, excluding retention rates.